Published in final edited form as:
Synapse. 2013 June ; 67(6): 265–279. doi:10.1002/syn.21637.

Deletion of the NMDA-NR1 receptor subunit gene in the mouse nucleus accumbens attenuates apomorphine-induced dopamine D1 receptor trafficking and acoustic startle behavior

Michael J. Glass[1,*], **Danielle C. Robinson**[1], **Elizabeth Waters**[2], and **Virginia M. Pickel**[1]
[1]Brain and Mind Research Institute, Weill Cornell Medical College, New York, NY 10065
[2]Laboratory of Neuroendocrinology, The Rockefeller University, NY, NY 10065

Abstract

The nucleus accumbens (Acb) contains subpopulations of neurons defined by their receptor content and potential involvement in sensorimotor gating and other behaviors that are dysfunctional in schizophrenia. In Acb neurons, the NMDA NR1 (NR1) subunit is co-expressed not only with the dopamine D1 receptor (D1R), but also with the μ-opioid receptor (μ-OR), which mediates certain behaviors that are adversely impacted by schizophrenia. The NMDA-NR1 subunit has been suggested to play a role in the D1R trafficking and behavioral dysfunctions resulting from systemic administration of apomorphine, a D1R and dopamine D2 receptor agonist that impacts prepulse inhibition (PPI) to auditory-evoked startle (AS). Together, this evidence suggests that the NMDA receptor may regulate D1R trafficking in Acb neurons, including those expressing μ-OR, in animals exposed to auditory startle and apomorphine. We tested this hypothesis by combining spatial-temporal gene deletion technology, dual labeling immunocytochemistry, and behavioral analysis. Deleting NR1 in Acb neurons prevented the increase in the dendritic density of plasma membrane D1Rs in single D1R and dual (D1R and μ-OR) labeled dendrites in the Acb in response to apomorphine and AS. Deleting NR1 also attenuated the decrease in AS induced by apomorphine. In the absence of apomorphine and startle, deletion of Acb NR1 diminished social interaction, without affecting novel object recognition, or open field activity. These results suggest that NR1 expression in the Acb is essential for apomorphine-induced D1R surface trafficking and reduction in AS, but also plays an independent role in controling social behaviors that are impaired in multiple psychiatric disorders.

Keywords

auditory startle; mu-opioid receptor; prepulse-inhibition; sociability; substance abuse

INTRODUCTION

Schizophrenia is characterized by deficits in cognitive (McNab et al. 2009) and motor function (Berthet et al. 2009), as well as in sensorimotor gating that is mediated in part through the nucleus accumbens (Acb; Ellenbroek, 2004; Amann et al., 2010). Systemic or local Acb administration of NMDA receptor antagonists elicits a similar gating deficit predominately through actions in the Acb core as compared with the Acb shell compartments (Wan and Swerdlow 1996a). While both Acb regions receive major glutamatergic input from the prefrontal cortex, the motor-associated, nucleus accumbens

[*]**Address correspondence to:** Dr. Michael J. Glass, Division of Neurobiology, Weill Cornell Medical College, 407 East 61st Street, New York, NY 10065, Phone: (646) 962-8253, FAX: (646) 962-0535, mjg2003@med.cornell.edu.

core also receives substantial glutamatergic input from the lateral amygdala as well as feed forward inhibition from the Acb shell, an important brain site involved in the integration of motivated behaviors (Zahm, 2000; Sesack and Grace, 2010).

The glutamatergic excitation of Acb neurons is potently modulated by dopamine activation of dopamine D1 and D2-like family of receptors (D1R and D2R; Rouillon et al., 2008). Apomorphine, a D1 and D2 receptor agonist, produces a reduction in prepulse inhibition (PPI) of the acoustic startle (AS) reflex in rodents, which is a reliable index of a sensorimotor gating deficit typical of many schizophrenics (Swerdlow et al. 2000; Wan and Swerdlow 1996b). It has been reported that exposure to apomorphine alone, or AS alone has no effect on the plasma membrane density of D1R in the Acb. However, the combination of apomorphine and AS has been associated with an increase the dendritic plasmalemmal density of D1Rs in spiny neurons of the Acb (Hara and Pickel 2007). The increase in surface D1R in these neurons may be at least partially dependent on activation of postsynaptic NMDA receptors. This hypothesis is suggested by the known physical protein-protein interactions between the cytoplasmic C-terminal domains of the D1R and the NMDA NR1 subunit (Lee et al. 2002; Pei et al. 2004).

The apomorphine and AS induced redistribution of D1Rs in the Acb shows region-specific differences in dendritic profiles that may be linked with their content of μ-opioid receptors (μ-ORs), which are frequently co-expressed with NMDA receptors in the Acb (Gracy et al., 2007). This is consistent with findings that μ-ORs are involved in several behaviors that are adversely impacted by schizophrenia (Havemann et al., 1983; Broderick et al., 1984; Angulo et al., 1991; Bertrand et al., 1997; Bortolato et al., 2005; Trezza et al., 2011). There is also co-morbidity between schizophrenia and the abuse of several addictive drugs (Chambers et al. 2001; Regier et al. 1990), the latter of which may significantly involve the activation of μ-OR (Zhang and Kelley, 2002; Scott et al., 2007; Simmons and Self, 2009) as well as dopamine release (Di Chiara and Imperato 1988) in the Acb. Despite these considerations, there is no evidence that AS or apomorphine specifically elicit changes in the distribution of D1R in subpopulations of Acb neurons that express μ-ORs, or that this trafficking is dependent on postsynaptic NMDA receptors. Additionally, the functional consequences of local NR1 gene deletion on AS and PPI are unknown.

We addressed these questions by combining conditional gene deletion technology and electron microscopic dual labeling of D1 and μ-OR in the Acb of adult mice receiving apomorphine or saline prior to AS. To gauge the role of Acb NR1 expression in behaviors beyond AS, and in the absence of apomorphine, cohorts of mice with Acb NR1 deletion were characterized with respect to behaviors commonly assayed in animal models of schizophrenia, including sociability and novel object recognition (Neill et al. 2010).

METHODS

Animals

Experimental protocols involving animals and their care were approved by the Institutional Animal Care and Use Committee at Weill Medical College of Cornell University and conformed to NIH guidelines. Forty-three adult (20–30 g) floxed NR1 (fNR1) male mice were given unilateral [electron microscopic analysis of apomorphine and AS, n=22] or bilateral [behavioral assessment without apomorphine, n=21] microinjections as described below. Mice homozygous for the fNR1 gene have loxP site placed in the intron that lies between exons 10 and 11 and a second site downstream after exon 22, the last exon (Glass et al., 2008; South et al. 2003). The two loxP sequences flank a region of the NR1 gene that encodes the 4 membrane domains and the entire C-terminal sequence of the polypeptide chain. These mice are maintained on the C57BL/6 background.

Viral vectors

A neurotropic serotype 2 recombinant adenoassociated virus (rAAV; ~4.7 kb; generously provided by Dr. Charles E. Inturrisi, Weill Cornell Medical College) engineered without viral coding sequences (South et al. 2003) was used to deliver Cre recombinase (Cre) to brain targets. The inserted transgenes included a promoter/enhancer (human cytomegalovirus immediate early gene [CMV]), a multiple cloning site for insertion of the green fluorescent protein (GFP) and Cre (rAAV-Cre) or exclusive GFP (rAAV-GFP) coding sequences, and poly A sequences. These were flanked by 145 base pair inverted terminal repeats necessary for rAAV replication and packaging. The Cre enzyme was directed to the nucleus and loxP sites by nuclear localization signals.

Virus administration

Under deep isoflurane anesthesia, approximately 250-300 nl of rAAV-Cre or rAAV-GFP (5×10^6 viral particles per μl) were injected into the Acb. Microinjections were made 1.2 mm anterior and 0.8 mm lateral to bregma, at a depth of 4.6 mm from the skull surface (Paxinos and Franklin 2000). For added verification of the specificity of the effects of gene deletion, virus was also administered in an area 1 mm posterior to this target in the area of the bed nucleus of the stria terminalis in a separate placement control (PC) group. For vector administration, microinjections were made by interfacing a picospritzer (Picospritzer II, General Valve Corp., Fairfield, NJ) to a glass pipette (WPI, Sarasota, FL), whose tip was pulled to a diameter of ~50 μm, via a pipette holder and plastic tubing. Injections were made over a 15-minute interval. In all cases, to prevent leakage of solution, the pipette was left in place for an additional 15-minutes. Bone wax was used to cover the bore-hole, and the mice were allowed to recover in their home cages. At least 14 days were required for maximal gene deletion (Glass et al. 2008).

AS/PPI treatment overview and electron microscopic immunolabeling

Drug administration and auditory testing—Baseline startle was measured one week prior to subcutaneous (sc) injection of apomorphine (5 mg/kg) or saline in rAAV-GFP-control and rAAV-Cre treated mice. These injections were given 5 minutes prior to auditory testing for PPI and AS described in the next section. This testing required approximately 14 minutes, and the animals were returned to their home cage for approximately 40 minutes so that 60 minutes elapsed between apomorphine or saline injection and perfusion fixation After fixation, brains were immediately sectioned and processing their brain tissue for immunolabeling.

Tissue fixation—Mice were anesthetized with pentobarbital (150 mg/kg, i.p.), and their brains were fixed by cardiac perfusion sequentially with: (a) 15 ml of normal saline (0.9%) containing 1000 units/ml of heparin, (b) 40 ml of 3.75% acrolein in 2% paraformaldehyde (PFA) in 0.1 M phosphate buffer (PB, pH 7.4), and (c) 100 ml of 2% PFA in PB, all delivered at a flow rate of 25 ml/minute. The brains were removed and post-fixed for 90-120 minutes in 2% PFA in PB. Coronal sections (40 μm) from the forebrain at the level of the Acb were cut with a vibrating microtome.

Antisera—A guinea pig anti-μ-OR antiserum (Chemicon, Temecula, CA) was raised against amino acids 384-398 of the cloned rat μ-OR. Immunolabeling of this receptor is abolished by preadsorption with the antigenic peptide (Drake and Milner 2002), and significantly attenuated in mice with a knockout of either exon 1, 2/3, or 11 of the μ-OR gene, respectively (Jaferi and Pickel 2009). The monoclonal rat anti-D1R antibody was raised against the C-terminus of the human D1R receptor (Clone 1-1-F11 S.E6, Sigma RBI, Saint Louis, MO). This antiserum has been shown to recognize the antigenic peptide by

Western Blotting, immunoprecipitation, and blocking control experiments, as well as mouse knockout models (Hara and Pickel 2005; Jaferi and Pickel 2009). A monoclonal mouse anti-NR1 antibody (Pharmingen, San Diego, CA) was used to label NR1; labeling for this antisera has been shown to be reduced following rAAV-Cre administration into the brain in fNR1 mice (Beckerman and Glass 2012; Glass et al. 2008). A previously characterized rabbit anti-GFP antisera (Invitrogen, Carlsbad, CA) was used to identify brain regions of viral mediated gene transfer (Glass et al,, 2008).

Immunoelectron microscopic dual labeling—Sections through the Acb of each of the experimental and control groups of mice were processed for dual immunolabeling as previously described (Chan et al. 1990; Leranth and Pickel 1989). Immunogold-silver was used for labeling the D1R to quantify the subcellular location of this protein, and μ-OR was identified using the immunoperoxidase method, which produces a robust diffuse reaction product that is readily distinguished from immunogold-silver. Tissue sections were placed in 1.0% sodium borohydride in PB for 30 minutes, washed in PB and immersed in room temperature cryoprotectant solution (20% sucrose and 8% glycerol in 0.05MPB) before freezing for 15 minutes in −80 °C. Sections were next rinsed in 0.1 M Tris-buffered saline (TBS, pH 7.6), and then incubated for 30 minutes in 0.5% BSA to minimize nonspecific labeling. Tissue sections were incubated in a cocktail of primary antisera containing rat anti-D1R antisera (1:50) and guinea pig anti-μ-OR (1:400) for 48 hours. Following the primary antisera incubation, sections were washed in TBS. Tissue sections processed for μ-OR immunoperoxidase labeling were incubated in anti-guinea pig IgG conjugated to biotin (1:400, 30 minutes) and rinsed in TBS. Tissue sections were then incubated for 30 minutes in avidin-biotin complex (ABC; Vector Laboratories, Burlingame CA) in TBS. The bound peroxidase was visualized by reaction for 6 minutes in 0.2% solution of 3,3′ diaminobenzidine (DAB; Sigma-Aldrich, St. Louis, MO) and 0.003% hydrogen peroxide in TBS. For immunogold labeling of D1R, sections were rinsed in 0.01 M phosphate buffered saline (PBS, pH 7.4), and blocked for 10 minutes in 0.8% BSA and 0.1% gelatin in PBS to reduce non-specific binding of gold particles. Sections were then incubated for 2 hours in anti-rat IgG conjugated with 0.6 nm gold particles (1:50, AuroProbeOne, Amersham, Arlington Heights, IL), and then rinsed in 0.5% BSA and 0.1% gelatin in PBS, followed PBS. After gold conjugated secondary antisera incubation, sections were incubated for 10 minutes in 2% glutaraldehyde in PBS, and then rinsed in PBS. The bound gold particles were enlarged by a 6-minute silver intensification using an IntenSE-M kit (Amersham, Arlington Heights, IL).

Electron microscopic tissue processing and figure preparation—For electron microscopic processing, the tissue was postfixed in 2% osmium tetroxide in PB for one hour, and dehydrated in a series of alcohols and propylene oxide before being flat embedded in EM BED 812 (EMS, Fort Washington, PA) between 2 sheets of Aclar plastic. Ultrathin sections (60-80 nm) from the surface of flat-embedded sections containing the ventral forebrain were cut with a diamond knife using a Leica EM UC6 ultratome (Leica Microsystems), and sections were collected on copper mesh grids. Electron microscopic images of this tissue were obtained using a digital camera (Advanced Microscopy Techniques, Danvers, MA) interfaced with a transmission electron microscope (Technai 12 BioTwin, FEI, Hillsboro, OR). For preparation of figures, images were adjusted for contrast and brightness using Adobe Photoshop CS4 software, and imported into Microsoft Office PowerPoint 2008 to add lettering and generate composite figures.

Ultrastructural analysis—In order to control for potential labeling artifacts due to penetration of cytological reagents, sampling was performed at the tissue surface as determined by proximity to the epon-tissue interface. This was achieved by collecting

electron micrographs exclusively in the transition zone (where one edge of the sampling area was in contact with epon in a field of at least three grid squares) and at a consistent depth from the surface. Digital images were captured and analyzed to determine the number of single and dual labeled neuronal profiles. Random systematic sampling of KO or control areas of Acb were performed as previously described (Hara and Pickel, 2008; Glass et. al. 2008). The classification of labeled neuronal profiles is based upon descriptions by Peters et. al. (Peters et al. 1991). Dendrites were identified by the presence of postsynaptic densities, as well as ribosomes and both rough and smooth endoplasmic reticulum. However, profiles also were considered dendritic whenever postsynaptic densities were observed, independent of endoplasmic reticulum. Somata were distinguished by the presence of a nucleus. Axon terminals were defined by size (at least 0.2 μm diameter) and the presence of synaptic vesicles. Synapses were defined as either symmetric or asymmetric, according to the presence of either thin or thick postsynaptic specializations, respectively. Appositions were distinguished by closely spaced plasma membranes that lacked recognizable specializations, or interposing astrocytic processes defined by their irregular shape and occasional presence of astrocytic filaments or gap junctions.

Immunoperoxidase labeling in electron microscopic images was distinguished by a diffuse black precipitate having an electron density greater than that seen in similar profiles within the neuropil. The immunogold-silver deposits appeared as dense uniformly black granules readily distinguishable from the peroxidase reaction product by visual inspection. With either the immunoperoxidase or immunogold method, perceived non-specific labeling was most commonly seen along the damaged membranes at the tissue surface, which were not included in the analysis. The scarcity of the spurious gold particles in our study is consistent with earlier reports that background contributes only about 3% or less of silver-enhanced gold particles (Wang et al. 2003).

Neuropil was assessed using MCID software to quantify cross-sectional area, perimeter, gold to membrane distance, etc. Data was pooled from animals in each treatment condition. Data were analyzed by one-or two-way factorial Analysis of Variance, and differences in means were analyzed by Tukey's HSD. JMP8 software was used for K-means cluster analysis; ANOVA and t-tests were used for statistical comparisons when appropriate.

Light microscopic immunocytochemistry and cell counting—To identify the extent of viral mediated gene transfer and NR1 gene deletion, a subsample of tissue sections adjacent to those processed for EM were processed for light microscopy. Brain sections were incubated for 24 hours in rabbit anti-GFP antiserum (1:1000), or 48 hours in a mouse anti-NR1 antibody (1:100) in 0.1% BSA. After incubation, sections were rinsed in 0.1 M TBS, incubated in anti-rabbit or anti-mouse IgG conjugated to biotin (1:400), rinsed in TBS, and then incubated for 30 minutes in ABC in TBS. The bound peroxidase was visualized by reaction for 6 minutes in 0.2% solution of DAB and 0.003% hydrogen peroxide in TBS. Following DAB incubation, sections were washed in 0.1% TBS, then 0.05 M PB, dehydrated through a series of alcohols and then mounted in resin beneath a glass coverslip.

To determine the placement of the injection site, the area and extent of labeling for GFP was identified visually, while the number of NR1 labeled cells in the injection area was quantified. Cell counting was performed using relative optical density measurements via Microcomputer Imaging Device software (MCID, Imaging Research Inc., Ontario, Canada), as previously described (Glass et al., 2008). Briefly, mounted sections were viewed with a Nikon Microphot-FX microscope (Nikon, Garden City, NY) equipped with a digital CoolSNAP camera (Photometrics, Huntington Beach, CA). The light microscopic images were acquired through an interface between the camera and a Macintosh computer. Pixel intensity thresholding procedures were performed as per manufacturer's guidelines.

Electronic images were imported into MCID, which automatically calculates a relative threshold level for each image, then adjusted using an object enhancement filter that maximizes the contrast between large objects and background. For NR1, cell counts were made from the Acb of injected and contra lateral hemispheres in three sections in the area of the injection site. The ratio of NR1 labeled cells in the injected and contra lateral hemispheres were calculated for each section and averaged for each animal, then analyzed by ANOVA. Cell counts were also performed manually to verify the consistency of automated tallies.

Behavioral testing

Acoustic startle and prepulse inhibition—The AS and PPI testing was performed in a one chamber SR-LAB startle apparatus with digital output (San Diego Instruments, San Diego CA), as previously described (Hara and Pickel 2007). The testing included a 76dB background noise (5 minutes) for acclimation; 120dB pulse alone (6 trials); and a pseudorandom sequence of 120dB pulse alone (10 trials), 79dB prepulse + 120dB pulse alone (5 trials), 82dB prepulse + 120dB pulse alone (5 trials), and 85dB prepulse + 120dB pulse alone (5 trials). All pulse alone trials were 100ms and the prepulse was 20ms.

Each mouse was handled daily for at least 5 minutes following surgical recovery, seven days prior to the apomorphine AS/PPI trial, animals were exposed to the AS/PPI stimulus to get a baseline for each animal and identify any abnormal responses. Three-minutes of habituation to the startle chamber began one week prior to the initial AS/PPI test, and continued between the baseline test and drug test. Animals were randomly assigned to apomorphine or vehicle control groups. When apomorphine treatment preceded the acoustic startle testing, animals were injected with 5 mg/kg of the agent 5 minutes before being placed in the startle apparatus to begin the testing as described above. Animals that received unilateral injections of the Cre or GFP for EM analysis were returned to their home cages for 40 minutes following startle testing and were sacrificed via cardiac perfusion 60 minutes after apomorphine or vehicle injection. Animals that received bilateral Cre of GFP injections were returned to their home cages with free access to food and water. For these animals, daily handling continued and one week elapsed before the next behavioral test.

Sociability test—Animals were introduced to a testing arena containing a novel male mouse in one corner of the arena. The novel mouse was an unfamiliar young male of the same “floxed” genetic background. Animals were observed and recorded for 15 minutes as they explored the arena. Video was analyzed using Noldus Ethovision XT V. 8 (Leesburg, VA). Latency to approach, frequency of approach, and time in close proximity to the novel mouse were assessed with respect to a 3 cm boundary zone around the container as well as direct contact. Arena and container were thoroughly cleaned between mice. Mice were handled daily prior to sociability test, but were not habituated to the testing arena.

Novel object recognition—A simple test design consisted of a 5 minute training session with two identical objects, a first test (Test 1) 3 hours later with one novel object, and a second test (Test 2) 24 hours later with another novel object. Animals were introduced to a testing arena with two identical objects on either side of the arena. Animals were then observed and filmed for 5 minutes while they explored the arena. Subsequent tests were similarly conducted except that one of the familiar objects was substituted with a novel object. Video files were analyzed using Noldus Ethovision XT V. 8 software. Duration, latency and frequency were assessed with respect to each half of the arena, a 3 cm boundary around each object, and contact with the objects themselves.

Locomotor activity—Locomotor behavior was observed using an open-field test chamber (Med Associates, Saint Albans, VT). Distance traveled, time ambulatory, time at rest, and time spent involved in stereotypic behavior were assessed over a 90-minute period and data were analyzed with Activity Monitor software. Mice were handled daily prior to locomotor activity assessment, but were not habituated to the open field.

RESULTS

Deleting NR1 in the Acb affects the AS response to apomorphine

Inhibiting NMDA receptor function by pharmacological (Nakaya et al. 2011) or constitutive genetic (Bickel et al. 2008) approaches has been shown to impact AS behavior in the mouse. However, the role of Acb NR1 gene expression in startle behaviors is unknown. To examine this issue, a local deletion of NR1 in the Acb was generated by microinjecting rAAV-Cre into the core or shell of the Acb in fNR1 mice. Separate mice were treated with the control rAAV-GFP vector. Both groups were subsequently tested for AS and PPI behavior after saline or apomorphine injections (Tables 1 and 2).

There was a significant reduction in auditory startle after apomorphine injection compared to saline [$F(1,8)= 16.3$, $p<0.004$; Fig. 1A] in mice injected with rAAV-GFP, although there was no significant difference in %PPI ($p>0.7$; Fig. 1B). Unlike the rAAV-GFP injected mice, animals receiving Acb rAAV-Cre did not show differences in AS ($p>0.09$; Fig. 1C), indicating that local deletion of the NR1 gene in the Acb prevented apomorphine-induced suppression of AS. Similar to the rAAV-GFP treated mice, rAAV-Cre treated animals did not differ in %PPI ($p>0.5$; Figure 1D) in response to apomorphine. There were no differences in either AS ($p>0.3$) or %PPI ($p>0.1$) in mice receiving rAAV-GFP in the core or shell subregions and subsequently treated with apomorphine, nor were there differences in AS ($p>0.2$) or %PPI ($p>0.9$) in apomorphine treated mice receiving rAAV-Cre injections in each respective Acb region.

Immunoperoxidase labeling for GFP identified the sites of virally mediated gene transfer in the Acb core (Fig. 2A) or shell (Fig. 2B) of fNR1 mice. Compared to rAAV-GFP treated mice, microinjection of rAAV-Cre resulted in a significant reduction of over 40% of NR1 immunoreactivity in the injected hemisphere relative to the contra lateral hemisphere [$F(1, 18) = 5$, $p<0.05$; Fig, 2C-F].

Apomorphine and AS result in an increase in dendritic D1R surface density in mice receiving rAAV-GFP in the Acb core

It has been shown that apomorphine given to rats subject to AS results in an increase in the dendritic plasmalemmal density of D1Rs in spiny neurons of the Acb (Hara and Pickel 2007). In order to determine the role of functional NMDA receptors in the subcellular location of D1Rs induced by apomorphine and AS, quantitaive immunogold electron microscopic analysis of D1R was performed in the Acb. Tissue was obtained from subgroups of the saline or apomorphine treated mice tested above for AS behavior. . Since NMDA receptors are frequently co-expressed with μ-ORs in the Acb (Gracy et al., 2007), and μ-ORs are also involved in several behaviors that are adversely impacted by schizophrenia (Trezza et al. 2011), tissue was processed for dual labeling of D1R and μ-OR, the latter serving as a functionally-relevant marker. We noted qualitative and quantitative differences in saline and apomorphine treated mice after AS testing with respect to the subcellulcar location of dendritic D1R in neurons in the Acb core, but not the shell, as discussed below.

Compared with mice receiving saline and exposed to AS (Fig. 3A, B), D1R immunogold particles were more commonly in contact with the plasmalemma of dendritic shafts in the Acb core of rAAV-GFP recipient mice receiving systemic administration of apomorphine and AS exposure (Fig. 3D, E) These differences were seen in dendritic profiles showing exclusive D1R immunoreactivity, as well as in those containing both D1R and μ-OR labeling. In addition, the μOR labeled dendritic spines also frequently appeared larger in the Acb core of the GFP control mice receiving apomorphine versus saline (Fig. 3F and 3C, respectively). Quantitative analysis further established the statistical significance of the increase in dendritic D1R plasmalemmal density (Fig. 3G) and size of the μ-OR labeled dendritic spines (Fig. 3H) in the Acb core of mice receiving apomorphine. Compared to mice receiving saline and AS, those exposed to apomorphine and AS had a significantly greater plasmalemmal D1R density in single [$F(1, 224)= 9.2$, $p<0.003$; Fig. 3G] and dual [$F(1, 412)=14.7$, $p>0.0001$; Fig. 3G] labeled dendrites, as well as single [$F(1, 78)=9.8$, $p<0.003$; Fig. 3G] and dual [$F(1, 70)=2.6$, $p>0.1$ n.s.; Fig. 3G] labeled dendritic spines. However, there were no significant differences in intracellular D1R in single ($p>0.2$) or dual D1R ($p>0.7$) labeled dendrites, nor in single ($p>0.4$) or dual ($p>.9$) labeled spines. Differences in surface or cross-sectional area were also not seen in single D1R or dual labeled profiles (Fig. 3H). In μ-OR labeled dendrites, there was no difference in profile size in the Acb of GFP saline/AS and apomorphine/AS treated mice ($n=515$, $p>0.6$; Fig. 3H). In contrast, in apomorphine/AS treated animals, dendritic spines expressing μ-opioid receptors in the Acb core were significantly larger [$F(1, 504)=8.5$, $p<0.004$; Fig. 3H] than those of saline/AS administered animals.

In the shell region of the Acb, there were no significant differences in the density of surface D1R in saline/AS and apomorphine/AS treated mice receiving rAAV-GFP. This was the case in single ($n= 74$, $p>0.6$) and dual ($n=302$, $p>0.1$) labeled dendrites, as well as single ($n=38$, $p>0.3$) and dual ($n=78$, $p>0.7$) labeled spines. Neither were there differences in the density of cytoplasmic D1R in single ($p>.8$) or dual ($p>.4$), labeled dendrites, nor in single ($n=36$, $p>.2$) or dual ($p>.3$) labeled spines. In addition, no differences were found in the area of μ-OR labeled dendrites ($n=744$, $p>.9$) or spines ($n=849$, $p>.1$).

Apomorphine and AS do not result in an increase in dendritic D1R surface density in the Acb core following local rAAV-Cre mediated NR1 deletion

In contrast with the extensive plasmalemmal distribution of D1R immunogold in dendrites and dendritic spines in the Acb core of apomorphine-treated rAAV-GFP mice (Fig. 4A), D1R labeling was less frequently observed on the plasma membrane of medium (Fig. 4B) and small (Fig. 4C) dendritic profiles in mice receiving rAAV-Cre injections in the Acb prior to apomorphine administration and AS testing.

Quantitative analysis in the Acb core revealed no significant difference between rAAV-Cre or rAAV-GFP mice exposed to apmorphine and AS with respect to the density of plasmalemmal D1R in single ($n=196$, $p>0.3$; Figure 4D), or dual ($n=482$, $p>0.4$; Fig. 4D) labeled dendrites, or in single ($n=141$, $p>0.4$; Fig. 4D) or dual ($n=150$, $p>0.4$; Fig. 4D) labeled spines. In addition, differences in intracellular D1R were not observed in single ($p>0.09$) or dual ($p>0.06$) labeled dendrites, nor in single ($p>0.5$) or dual ($p>0.6$) labeled spines. Surface and cross-sectional areas were comparable between treatment groups except for a decrease in the cross-sectional area of dual labeled dendritic shafts [$F(1, 481)=12.2$, $p=0.005$; Fig. 4E]. In single μOR labeled dendritic profiles, there were no significant differences in the cross-sectional area of dendrites ($n=553$, $p>0.1$; Fig. 4E) or spines ($n=478$, $p>0.1$; Fig. 4E). In sum, the contrasting surface levels of D1R, as well as the differences in μOR spine morphology seen in response to apomorphine and AS in control and Acb NR1 KO mice suggests that local NR1 expression is necessary for AS and D1/D2 receptor

agonist induced plasmalemmal D1R trafficking and the size of μOR expressing spines in the Acb core.

In the shell of the Acb, mice receiving rAAV-Cre and saline or apomorphine showed no significant differences in surface D1R in single (n=88, p>0.5) or dual (n=246, p>0.09) labeled dendritic profiles, nor in single (n=26, p>0.3) or dual (n=77, p>0.4) labeled spines. There were also no significant differences in the density of cytoplasmic D1R in single (p>0.2) or dual (p>0.3) labeled dendritic profiles, or single (p>0.3) or dual (p>0.9) labeled spines. No differences in the area of single D1R (dendrites: p>0.1; spines: p>0.1) or dual (dendrites: p>0.4; spines: p>0.5) labeled profiles, or single μOR labeled profiles (dendrites: n=779, p>0.9; spines: n=819, p>0.9) were seen.

Deletion of NR1 in the Acb impairs sociability without affecting object recognition or locomotor activity

In addition to sensory-motor processing, functional NMDA receptors have also been shown to play an important role in social behaviors (Duncan et al. 2004; Tanaka et al. 2003) and cognitive function (Smith-Roe et al. 1999), including object recognition (Smith et al. 2009). In order to flesh out our grasp of the role of Acb NMDA receptors in these behaviors, particularly in the absence of apomorphine, we examined the effect of Acb NR1 deletion on sociability, object recognition, and open field behavior.

We tested the effect of Acb NR1 deletion on social behavior in a social interaction task. There was a significant effect of treatment on the amount of time animals remained in contact with a novel mouse [$F(2, 16)=3.7$, $p<0.05$; Fig. 5A]. Compared to the Acb rAAV-GFP treated mice, animals receiving Acb rAAV-Cre spent significantly less time in contact with (Acb rAAV-Cre: 136.4±65, Acb rAAV-GFP: 223.8±55.3, $p<0.05$), and oriented toward (Acb rAAV-Cre: 429±22.4, Acb rAAV-GFP: 533.1±49.9, $p<0.05$) a novel mouse. In addition, compared to the Acb rAAV-GFP injected mice, animals receiving Acb injections of rAAV-Cre spent significantly less time in the quadrant housing the novel mouse (Acb rAAV-Cre: 451±90.7, Acb rAAV-GFP: 565.9±112.6, $p<0.05$). The latency to enter the novel mouse zone was also higher in Acb rAAV-Cre mice (Fig. 5B), although the latter failed to reach statistical significance (Acb rAAV-Cre: 138.3±29.6, Acb rAAV-GFP: 56.8±20.3, $p=.08$). There were no significant differences between Acb rAAV-Cre and PC rAAV-Cre mice (Fig. 5A, B), indicating that NR1 expression in sites outside the Acb also play a role in social interaction.

To assess episodic memory, animals were tested for visual recognition in the novel object recognition test, also in the absence of apomorphine. There were no significant differences between treatment groups in the amount of time spent in contact with either of two objects during the familiarization period [obj. 1: $F(2,15)=.3$, $p>0.7$; obj.2 $F(2, 15)= 1.9$, $p>0.1$; Fig 6]. In the recognition test animals were presented with one familiar object chosen from the initial familiarization trial and a novel object. The Acb rAAV-Cre and Acb rAAV-GFP injected mice spent significantly more time with the novel object versus the familiar object [difference score (novel – familiar obj):, Acb rAAV-Cre: 58.6±132.6, Acb rAAV-GFP: 58.2±95.9, $p<0.05$; Figure 6], although this was not the case with the PC rAAV-Cre injected animals (−28.6±15.8).

The effect of Acb NR1 deletion on locomotor behavior was investigated by measuring activity levels in an automated open field. There were no differences in the total distance traveled [$F(2, 27)=.9$, $p>0.4$; Fig. 7A] or total ambulatory time (Fig. 7B) between Acb rAAV-Cre, Acb rAAV-GFP, and PC rAAV-Cre injected animals.

DISCUSSION

These results provide the first evidence that neuronal NR1 gene expression in the Acb core is a key determinant of the dendritic partitioning of D1Rs in response to apomorphine and AS. Moreover, behavioral testing of mice with Acb NR1 deletion inclusive of both the Acb shell and core revealed that local neuronal NR1 gene expression is required for the normal expression of AS, as well as sociability. These results are discussed along with important methodological considerations and implications for understanding the pathophysiology of schizophrenia.

Methodological Considerations

The impact of NR1 gene deletion on apomorphine and AS induced D1R trafficking in the nucleus accumbens was separately examined in NR1 floxed mice having viral injections that preferentially targeted the medial Acb shell or core compartments. However, there was often partial overlap of the injections in these compartments, and there is substantial feed-forward of information from the Acb shell to the core (Zahm, 2000). Thus, we can not exclude the possibility that at least some of the anatomical changes reported in the Acb core are secondary to effects of NR1 gene deletion in the Acb shell. The functional relevance of NMDA receptors in both regions is strongly supported by the behavioral analysis in which viral injections in the Acb core and/or shell were equally effective in the selective reduction of AS in the NR1 floxed mice.

Apomorphine and AS result in an increase in the density of dendritic plasmalemmal D1R in the Acb core

Apomorphine administration was associated with a marked increase in D1R surface density in dendrites located preferentially in the Acb core. The increased plasmalemmal distribution of the D1R immunogold labeling likely represents functional receptors, since a correspondence between binding sites and surface labeling has been shown in other receptor systems (Boudin et al., 1998). The regional specificity of the apomorphine and AS-induced D1R redistribution in the mouse Acb core seen in the present study differs from the more pronounced effect of apomorphine on D1R distribution in dendritic spines the Acb shell of the rat (Hara and Pickel, 2007). This species difference is consistent with the known species variation between rat and mouse in their behavioral responses to apomorphine (Ralph-Williams et al. 2002; Varty et al. 2001).

Local Acb NR1 deletion prevents the increase in dendritic D1R surface density in the Acb core of mice exposed to apomorphine and AS

Compared to Acb rAAV-GFP injected mice, Acb rAAV-Cre injected animals exposed to AS and apomorphine did not show an increase in plasma membrane D1R labeling in dendritic profiles in the Acb core. These results indicate that local expression of the NR1 gene, and, presumably, functional NMDA receptors, play an important role in determing the surface availability of D1R in dendrites of Acb core neurons in response to AS and apomorphine.

In general, changes in the spatial pattern of D1R labeling may be mediated by any number of processes known to impact the surface and intracellular availability of this receptor. These include protein synthesis (Ohtsuka et al. 2008), endoplasmic reticula retention and plasmalemmal incorporation (Bermak et al. 2001; Kong et al. 2006), receptor binding by agonist (Dumartin et al. 2000), as well as endocytosis (Kotowski et al. 2011; Zhang et al. 2007), recycling (Martin-Negrier et al. 2006; Vargas and Von Zastrow 2004), or degradation. In this light, there is evidence that NMDA receptor activation influences a number of stages in the life cycle of D1R, including protein-protein heterodimerization and

protein trafficking (Scott et al. 2002)., and deletion of NR1 may thus inhibit the surface transport of the NMDA receptor by at least one of these mechanisms.

Apomorphine and AS elicit NMDA receptor-dependent structural changes in dendritic spines of Acb core neurons expressing μ-OR

There was a preferential increase in the size of μ-OR containing spines in the Acb core of AS and apomorphine treated rAAV-GFP mice, an effect not seen in animals receiving rAAV-Cre and apomorphine. These results indicate that functional NMDA receptors are required for alterations in the morphology of μOR expressing spines in response to AS and apomorphine. Inhibiting functional NMDA receptors has been shown to produce varying effects on spine morphology (Dang et al. 2006; Rampon et al. 2000), motility (Alvarez et al. 2007), and synapse formation (Adesnik et al. 2008). These variable relationships between NMDA receptors and dendritic spine morphology are consistent with the hypothesis that the dynamics of spine formation, motility, and retraction, rather than exclusive changes in total number, are essential for experience-dependent spine-related changes in neuronal information processing and plasticity (McKinney 2010). Therefore, in this context, the NMDA receptor dependent morphological changes in μ-OR expressing postsynaptic structures may be associated with alterations in the computational properties of spines (Yuste 2011). Such changes may have some relevance for the altered dendritic morphology (Penzes et al. 2011) and dysregulation of neuronal computational processes (Migliore et al. 2011) implicated in schizophrenia.

NR1 deletion in the Acb impairs AS after apomorphine

Impairing NMDA receptor function in Acb neurons also had an impact on AS behavior. Prior studies have shown that inhibiting NMDA receptor function by pharmacological (Curzon and Decker, 1998; Furuya et al., 1999; Yee et al., 2004; Kanahara et al., 2008; Nakaya et al., 2011) or constitutive genetic (Duncan et al., 2004; Fradley et al., 2005; Duncan et al., 2006; Moy et al., 2006; Bickel et al., 2008) approaches can produce diverse effects on startle and sensorimotor gating in the mouse. The reasons for this are unclear, but may involve the complex pharmacology of NMDA receptor antagonists, as well as the differential compensatory adaptations (Kew et al., 2000; Ballard et al., 2002) associated with constitutive genetic models. In the present study we spatially and temporally deleted the NR1 gene in neurons of the Acb in adult fNR1 animals by local intracranial delivery of a neurotropic rAAV expressing Cre recombinase (Beckerman and Glass 2012; Glass et al. 2008). This restricted deletion was associated with a reduction in apomorphine induced AS, but not PPI. These results demonstrate that the presence of the NR1 gene in Acb neurons is required for the normal expression of a behavioral reaction induced by an acoustic stimulus, but not for the auditory prepulse inhibition of the startle reaction. The lack of a significant difference in AS behavior when rAAV-Cre was administered in the Acb core compared with the shell suggests that the execution of these behaviors is equally dependent on NMDA receptor mediated transmission in both regions and potentially involves a flow-through of information from the Acb shell to the core (Zahm, 2000).

Acb NR1 deletion disrupts social interaction

Our results provide new evidence that NMDA receptors in the Acb are critical for social interactions. These results are consistent with the altered social behaviors resulting from pharmacological (Silvestre et al., 1997; Morimoto et al., 2002; Tanaka et al., 2003) or constitutive genetic (Duncan et al. 2004; Mohn et al. 1999) manipulations of the NMDA receptor. Unlike the actions of NMDA receptor antagonists (Koros et al. 2007) or mutant mice (Halene et al. 2009), the presently observed reduction in social interactions resulting from a spatial-temporal deletion of NR1 in the Acb are likely not attributable to a deficit in sensory processes or activity/exploratory behaviors. Moreover, the effect of Acb NR1

deletion on μ-OR expressing spine morphology and social behavior is consistent with a role for μ-OR in sociability in rodents (Wohr et al. 2011) and humans (Troisi et al. 2011), as well as the emerging role of Acb opioid receptors in social reward (Trezza et al. 2011).

Schizophrenia is associated with marked dysfunction of perceptual and cognitive processes that involve the Acb and related limbic forebrain circuits (Humphries and Prescott 2010). Activation of NMDA receptors in the Acb has been shown to play a role in behaviors critically involving the encoding, processing, recognition, and retrieval of sensory stimuli, including reward-related instrumental learning (Hernandez et al. 2005), approach behavior (Di Ciano et al. 2001), set shifting (Floresco et al. 2006), and spatial learning (Smith-Roe et al. 1999). However, in the present study, an object recognition paradigm was used to demonstrate that Acb NR1 deletion does not impact object recall.

Conclusions

The present findings indicate that Acb core NR1 expression is necessary for the modulation of local D1R surface trafficking in response to combined apomorphine and AS exposure. However, the functional relevance of NMDA receptors in neurons of both the Acb shell and core compartments is demonstrated by the selective reduction in acoustic startle behavior and social interactions resulting from NR1 gene deletion in either Acb subdivision. The inability of local NR1 deletion in Acb shell or core to impact PPI, novel object recognition, or open field activity suggests that these complex behaviors are not dependent on NMDA receptor mediated glutamatergic transmission in the Acb.

Acknowledgments

This research was supported by NIH grants: MH40342 and DA04600 to VMP and DA024030 and DA027128 to MJG. We are grateful to Andrea Gonzales for assistance with sociability and novel object quantification and to Eli Shobin and Eugene Ogorodnik for technical assistance.

REFERENCES

Adesnik H, Li G, During MJ, Pleasure SJ, Nicoll RA. NMDA receptors inhibit synapse unsilencing during brain development. PNAS. 2008; 105:5597–5602. [PubMed: 18375768]

Alvarez VA, Ridenour DA, Sabatini BL. Distinct structural and ionotropic roles of NMDA receptors in controlling spine and synapse stability. J. Neurosci. 2007; 27:7365–76. [PubMed: 17626197]

Beckerman MA, Glass MJ. The NMDA-NR1 receptor subunit and the mu-opioid receptor are expressed in somatodendritic compartments of central nucleus of the amygdala neurons projecting to the bed nucleus of the stria terminalis. Exp. Neurol. 2012; 234:112–126. [PubMed: 22227057]

Bermak JC, Li M, Bullock C, Zhou QY. Regulation of transport of the dopamine D1 receptor by a new membrane-associated ER protein. Nat. Cell Biol. 2001; 3:492–8. [PubMed: 11331877]

Berthet A, Porras G, Doudnikoff E, Stark H, Cador M, Bezard E, Bloch B. Pharmacological analysis demonstrates dramatic alteration of D1 dopamine receptor neuronal distribution in the rat analog of L-DOPA-induced dyskinesia. J. Neurosci. 2009; 29:4829–35. [PubMed: 19369551]

Bickel S, Lipp H-P, Umbricht D. Early auditory sensory processing deficits in mouse mutants with reduced NMDA receptor function. Neuropsychopharmacol. 2008; 33:1680–9.

Boudin H, Pelaprat D, Rostene W, Pickel VM, Beaudet A. Correlative ultrastructural distribution of neurotensin receptor proteins and binding sites in the rat substantia nigra. J. Neurosci. 1998; 18:8473–84. [PubMed: 9763490]

Chambers RA, Krystal JH, Self DW. A neurobiological basis for substance abuse comorbidity in schizophrenia. Biol. Psychiatry. 2001; 50:71–83. [PubMed: 11526998]

Chan J, Aoki C, Pickel VM. Optimization of differential immunogold-silver and peroxidase labeling with maintenance of ultrastructure in brain sections before plastic embedding. J. Neurosci. Methods. 1990; 33:113–127. [PubMed: 1977960]

Dang MT, Yokoi F, Yin HH, Lovinger DM, Wang Y, Li Y. Disrupted motor learning and long-term synaptic plasticity in mice lacking NMDAR1 in the striatum. PNAS. 2006; 103:15254–9. [PubMed: 17015831]

Di Chiara G, Imperato A. Drugs abused by humans preferentially increase synaptic dopamine concentrations in the mesolimbic system of freely moving rats. PNAS. 1988; 85:5274–8. [PubMed: 2899326]

Di Ciano P, Cardinal RN, Cowell RA, Little SJ, Everitt BJ. Differential involvement of NMDA, AMPA/kainate, and dopamine receptors in the nucleus accumbens core in the acquisition and performance of pavlovian approach behavior. J. Neurosci. 2001; 21:9471–7. [PubMed: 11717381]

Drake CT, Milner TA. Mu opioid receptors are in discrete hippocampal interneuron subpopulations. Hippocampus. 2002; 12:119–36. [PubMed: 12000113]

Dumartin B, Jaber M, Gonon F, Caron MG, Giros B, Bloch B. Dopamine tone regulates D1 receptor trafficking and delivery in striatal neurons in dopamine transporter-deficient mice. PNAS. 2000; 97:1879–84. [PubMed: 10677550]

Duncan GE, Moy SS, Perez A, Eddy DM, Zinzow WM, Lieberman JA, Snouwaert JN, Koller BH. Deficits in sensorimotor gating and tests of social behavior in a genetic model of reduced NMDA receptor function. Behav. Brain Res. 2004; 153:507–19. [PubMed: 15265649]

Floresco SB, Ghods-Sharifi S, Vexelman C, Magyar O. Dissociable roles for the nucleus accumbens core and shell in regulating set shifting. J. Neurosci. 2006; 26:2449–57. [PubMed: 16510723]

Glass MJ, Hegarty DM, Oselkin M, Quimson L, S.M. S, Xu Q, Pickel VM, Inturrisi CE. Conditional deletion of the NMDA-NR1 receptor subunit gene in the central nucleus of the amygdala inhibits naloxone-induced conditioned place aversion in morphine dependent mice. Exp. Neurol. 2008; 213:57–70. [PubMed: 18614169]

Halene TB, Ehrlichman RS, Liang Y, Christian EP, Jonak GJ, Gur TL, Blendy JA, Dow HC, Brodkin ES, Schneider F, Gur RC, Siegel SJ. Assessment of NMDA receptor NR1 subunit hypofunction in mice as a model for schizophrenia. Genes Brain Behav. 2009; 8:661–75. [PubMed: 19563516]

Hara Y, Pickel VM. Overlapping intracellular and differential synaptic distributions of dopamine D1 and glutamate N-methyl-D-aspartate receptors in rat nucleus accumbens. J. Comp. Neurol. 2005; 492:442–55. [PubMed: 16228995]

Hara Y, Pickel VM. Dendritic distributions of dopamine D1 receptors in the rat nucleus accumbens are synergistically affected by startle-evoking auditory stimulation and apomorphine. Neurosci. 2007; 146:1593–605.

Hernandez PJ, Andrzejewski ME, Sadeghian K, Panksepp JB, Kelley AE. AMPA/kainate, NMDA, and dopamine D1 receptor function in the nucleus accumbens core: a context-limited role in the encoding and consolidation of instrumental memory. Learning and Memory. 2005; 12:285–95. [PubMed: 15930507]

Humphries MD, Prescott TJ. The ventral basal ganglia, a selection mechanism at the crossroads of space, strategy, and reward. Prog. Neurobiol. 2010; 90:385–417. [PubMed: 19941931]

Jaferi A, Pickel VM. Mu-opioid and corticotropin-releasing-factor receptors show largely postsynaptic co-expression,and separate presynaptic distributions, in the mouse central amygdala and bed nucleus of the stria terminalis. Neurosci. 2009; 159:526–39.

Kong MM, Fan T, Varghese G, O'Dowd BF, George SR. Agonist-induced cell surface trafficking of an intracellularly sequestered D1 dopamine receptor homo-oligomer. Mol. Pharmacol. 2006; 70:78–89. [PubMed: 16597839]

Koros E, Rosenbrock H, Birk G, Weiss C, Sams-Dodd F. The selective mGlu5 receptor antagonist MTEP, similar to NMDA receptor antagonists, induces social isolation in rats. Neuropsychopharmacol. 2007; 32:562–76.

Kotowski SJ, Hopf FW, Seif T, Bonci A, von Zastrow M. Endocytosis promotes rapid dopaminergic signaling. Neuron. 2011; 71:278–90. [PubMed: 21791287]

Lee FJ, Xue S, Pei L, Vukusic B, Chery N, Wang Y, Wang YT, Niznik HB, Yu XM, Liu F. Dual regulation of NMDA receptor functions by direct protein-protein interactions with the dopamine D1 receptor. Cell. 2002; 111:219–30. [PubMed: 12408866]

Leranth, C.; Pickel, VM. Electron microscopic pre-embedding double immunostaining methods. In: Heimer, L.; Zaborszky, L., editors. Tract tracing methods 2, recent progress. Plenum; New York: 1989. p. 129-172.

Martin-Negrier ML, Charron G, Bloch B. Receptor recycling mediates plasma membrane recovery of dopamine D1 receptors in dendrites and axons after agonist-induced endocytosis in primary cultures of striatal neurons. Synapse. 2006; 60:194–204. [PubMed: 16739117]

McKinney RA. Excitatory amino acid involvement in dendritic spine formation, maintenance and remodelling. J. Physiol. 2010; 588:107–16. [PubMed: 19933758]

McNab F, Varrone A, Farde L, Jucaite A, Bystritsky P, Forssberg H, Klingberg T. Changes in cortical dopamine D1 receptor binding associated with cognitive training. Science. 2009; 323:800–2. [PubMed: 19197069]

Migliore M, De Blasi I, Tegolo D, Migliore R. A modeling study suggesting how a reduction in the context-dependent input on CA1 pyramidal neurons could generate schizophrenic behavior. Neural Networks. 2011; 24:552–9. [PubMed: 21315555]

Mohn AR, Gainetdinov RR, Caron MG, Koller BH. Mice with reduced NMDA receptor expression display behaviors related to schizophrenia. Cell. 1999; 98:427–36. [PubMed: 10481908]

Nakaya K, Nakagawasai O, Arai Y, Onogi H, Sato A, Niijima F, Tan-No K, Tadano T. Pharmacological characterizations of memantine-induced disruption of prepulse inhibition of the acoustic startle response in mice: involvement of dopamine D2 and 5-HT2A receptors. Behav. Brain Res. 2011; 218:165–73. [PubMed: 21130810]

Neill JC, Barnes S, Cook S, Grayson B, Idris NF, McLean SL, Snigdha S, Rajagopal L, Harte MK. Animal models of cognitive dysfunction and negative symptoms of schizophrenia: focus on NMDA receptor antagonism. Pharmacol. Therap. 2010; 128:419–32. [PubMed: 20705091]

Ohtsuka N, Tansky MF, Kuang H, Kourrich S, Thomas MJ, Rubenstein JL, Ekker M, Leeman SE, Tsien JZ. Functional disturbances in the striatum by region-specific ablation of NMDA receptors. PNAS. 2008; 105:12961–6. [PubMed: 18728179]

Paxinos, G.; Franklin, KB. The mouse brain in stereotaxic coordinates. Academic Press, Academic Press; 2000.

Pei L, Lee FJ, Moszczynska A, Vukusic B, Liu F. Regulation of dopamine D1 receptor function by physical interaction with the NMDA receptors. J. Neurosci. 2004; 24:1149–58. [PubMed: 14762133]

Penzes P, Cahill ME, Jones KA, VanLeeuwen JE, Woolfrey KM. Dendritic spine pathology in neuropsychiatric disorder. Nature Neurosci. 2011; 14:285–93. [PubMed: 21346746]

Peters, A.; Palay, SL.; Webster, H. The fine structure of the nervous system. Oxford University Press, Oxford University Press; 1991.

Ralph-Williams RJ, Lehmann-Masten V, Otero-Corchon V, Low MJ, Geyer MA. Differential effects of direct and indirect dopamine agonists on prepulse inhibition: a study in D1 and D2 receptor knock-out mice. J. Neurosci. 2002; 22:9604–11. [PubMed: 12417685]

Rampon C, Tang Y-P, Goodhouse J, Shimizu E, Kyln M, Tsien JZ. Enrichment induces structural changes and recovery from nonspatial memory deficits in CA1 NMDAR1-knockout mice. Nat. Neurosci. 2000; 3:238–244. [PubMed: 10700255]

Regier DA, Farmer ME, Rae DS, Locke BZ, Keith SJ, Judd LL, Goodwin FK. Comorbidity of mental disorders with alcohol and other drug abuse. Results from the Epidemiologic Catchment Area (ECA) Study. JAMA. 1990; 264:2511–8. [PubMed: 2232018]

Scott L, Kruse MS, Forssberg H, Brismar H, Greengard P, Aperia A. Selective upregulation of dopamine D1 receptors in dendritic spines by NMDA receptor activation. PNAS. 2002; 99:1661–1664. [PubMed: 11818555]

Smith SM, Uslaner JM, Yao L, Mullins CM, Surles NO, Huszar SL, McNaughton CH, Pascarella DM, Kandebo M, Hinchliffe RM, Sparey T, Brandon NJ, Jones B, Venkatraman S, Young MB, Sachs N, Jacobson MA, Hutson PH. The behavioral and neurochemical effects of a novel D-amino acid oxidase inhibitor compound 8 [4H-thieno [3,2-b]pyrrole-5-carboxylic acid] and D-serine. J. Pharmacol. Exp.Ther. 2009; 328:921–30. [PubMed: 19088300]

Smith-Roe SL, Sadeghian K, Kelley AE. Spatial learning and performance in the radial arm maze is impaired after N-methyl-D-aspartate (NMDA) receptor blockade in striatal subregions. Behav. Neurosci. 1999; 113:703–17. [PubMed: 10495079]

Swerdlow NR, Braff DL, Geyer MA. Animal models of deficient sensorimotor gating: what we know, what we think we know, and what we hope to know soon. Behav. Pharmacol. 2000; 11:185–204. [PubMed: 11103873]

Tanaka K, Suzuki M, Sumiyoshi T, Murata M, Tsunoda M, Kurachi M. Subchronic phencyclidine administration alters central vasopressin receptor binding and social interaction in the rat. Brain Res. 2003; 992:239–45. [PubMed: 14625062]

Trezza V, Damsteegt R, Achterberg EJ, Vanderschuren LJ. Nucleus accumbens mu-opioid receptors mediate social reward. J. Neurosci. 2011; 31:6362–70. [PubMed: 21525276]

Troisi A, Frazzetto G, Carola V, Di Lorenzo G, Coviello M, D'Amato FR, Moles A, Siracusano A, Gross C. Social hedonic capacity is associated with the A118G polymorphism of the mu-opioid receptor gene (OPRM1) in adult healthy volunteers and psychiatric patients. Social Neurosci. 2011; 6:88–97.

Vargas GA, Von Zastrow M. Identification of a novel endocytic recycling signal in the D1 dopamine receptor. J. Biol. Chem. 2004; 279:37461–9. [PubMed: 15192107]

Varty GB, Walters N, Cohen-Williams M, Carey GJ. Comparison of apomorphine, amphetamine and dizocilpine disruptions of prepulse inhibition in inbred and outbred mice strains. Eur. J. Pharmacol. 2001; 424:27–36. [PubMed: 11470257]

Wan FJ, Swerdlow NR. Sensorimotor gating in rats is regulated by different dopamine-glutamate interactions in the nucleus accumbens core and shell subregions. Brain Res. 1996a; 722:168–76. [PubMed: 8813362]

Wan FJ, Swerdlow NR. Sensorimotor gating in rats is regulated by different dopamine-glutamate interactions in the nucleus accumbens core and shell subregions. Brain Res. 1996b; 722:168–76. [PubMed: 8813362]

Wang H, Cuzon VC, Pickel VM. Postnatal development of mu-opioid receptors in the rat caudate-putamen nucleus parallels asymmetric synapse formation. Neurosci. 2003; 118:695–708.

Wohr M, Moles A, Schwarting RK, D'Amato FR. Lack of social exploratory activation in male mu-opioid receptor KO mice in response to playback of female ultrasonic vocalizations. Social Neurosci. 2011; 6:76–87.

Yuste R. Dendritic spines and distributed circuits. Neuron. 2011; 71:772–81. [PubMed: 21903072]

Zhang J, Vinuela A, Neely MH, Hallett PJ, Grant SG, Miller GM, Isacson O, Caron MG, Yao WD. Inhibition of the dopamine D1 receptor signaling by PSD-95. J. Biol. Chem. 2007; 282:15778–89. [PubMed: 17369255]

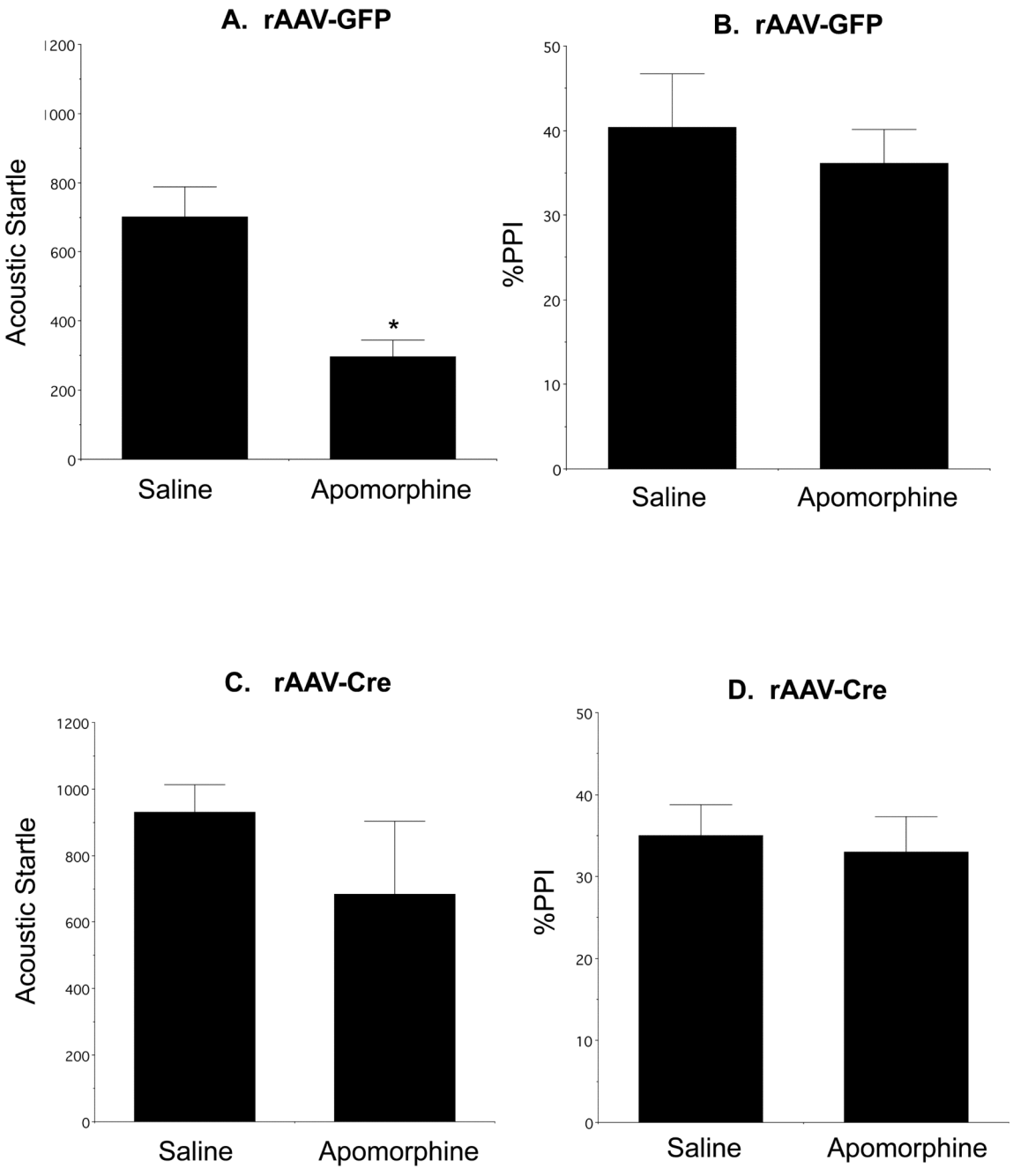

Figure 1.

NR1 deletion in the Acb attenuates the normal apomorphine-induced reduction in the peak amplitude of auditory-evoked startle. Apomorphine results in a reduction in AS **(A)** but not %PPI **(B)** in fNR1 mice receiving Acb rAAV-GFP. There is no reduction in AS **(C)** or %PPI **(D)** in fNR1 mice receiving rAAV-Cre in the Acb. *p<0.05, saline versus apomorphine in Acb rAAV-GFP injected mice by Fisher's PLSD.

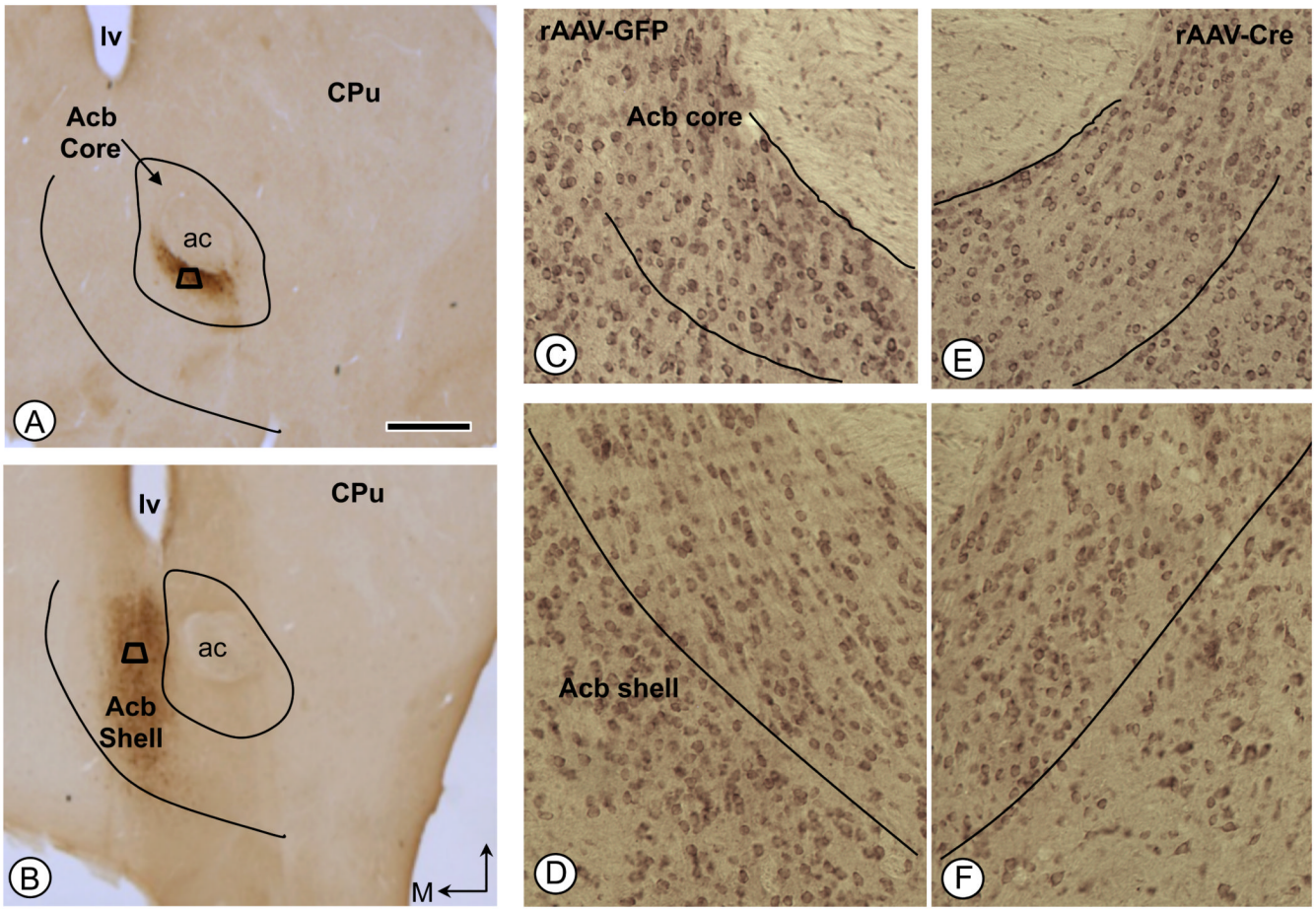

Figure 2.

Immunoperoxidase labeling of the GFP reporter protein in the Acb following local unilateral microinjection of vector into either the core **(A)** or shell **(B)** subregions. Areas bounded by the trapezoids represent regions where tissue was sampled by EM in adjacent sections processed for dual D1R and μ-OR immunolabeling. **(C-F)**. NR1 immunolabeling in the Acb core **(C, E)** and shell **(D, F)** of rAAV-GFP and rAAV-Cre injected mice, respectively. Bar=500 μm ac: anterior commissure, CPu: caudate-putamen, D: dorsal, lv: lateral ventricle; M: medial.

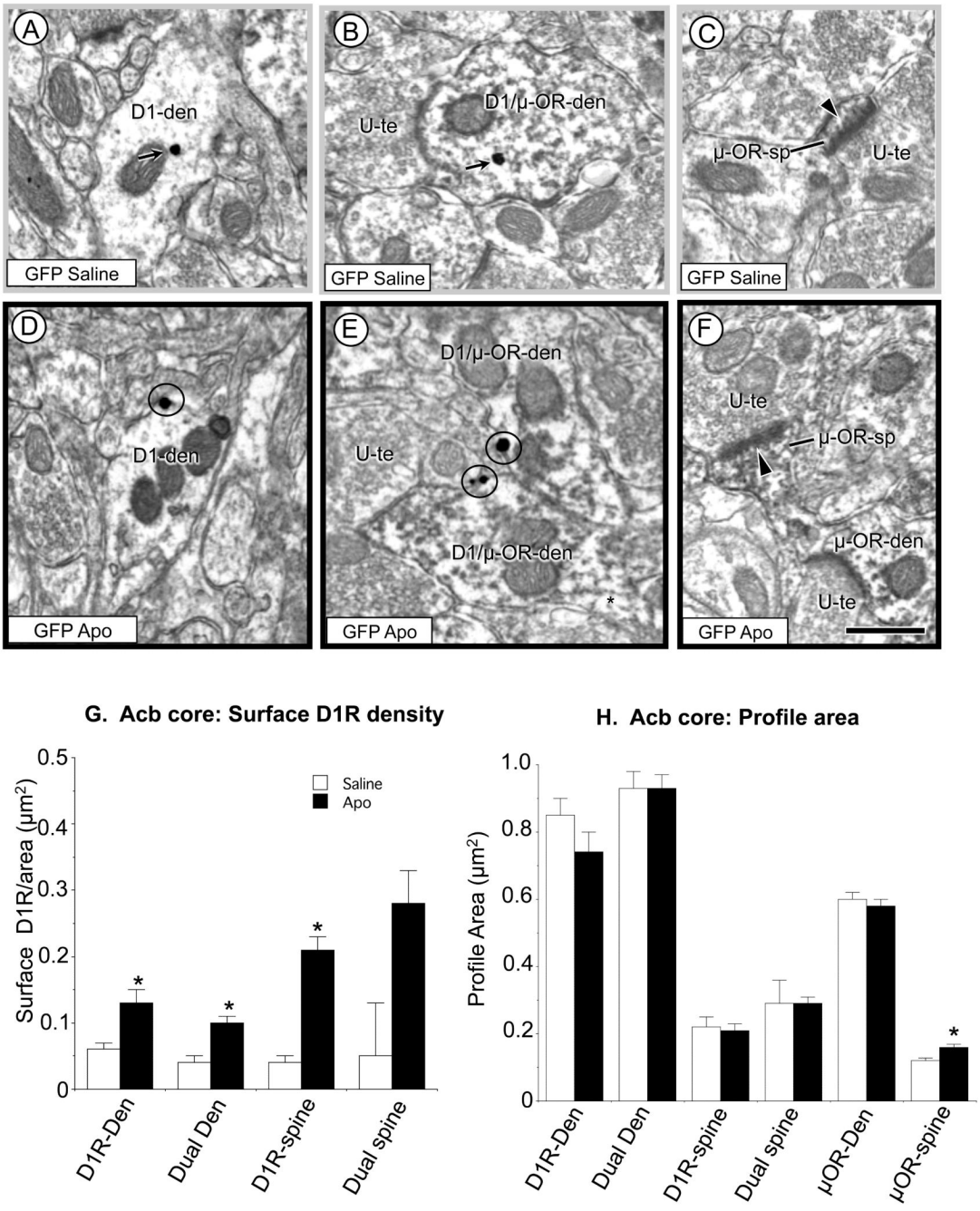

Figure 3.

Immunogold D1R and immunoperoxidase μ-OR labeling in the Acb core of mice receiving rAAV-GFP and treated with saline (n=3) or apomorphine (Apo, n=3) and tested for AS. In electron micrographs from the saline-treatment group **(A-B)** the dendritic D1R immunogold particles have a largely cytoplasmic distribution (arrows). In those receiving apomorphine **(D-E)** D1R immunogold particles show a plasmalemmal location (circles) in single (D1-den) and dual labeled D1R/μ-OR-den dendrites (D1/μ-OR-den). In both the saline and apomorphine treated mice, μ-OR containing dendritic spines (μOR-sp) receive asymmetric excitatory-type synapses (arrow heads) from unlabeled terminals (U-te), but the

representative dendritic spines appear larger in the mice receiving apomorphine **(F)** compared with those receiving saline **(C)**. In **G**, the bar graph shows a significant increase in surface labeling in single D1R and dual labeled dendritic shafts, as well as D1R labeled spines. In **H**, there is a significant increase in the cross-sectional area of μ-OR labeled spines in the Acb core of apomorphine treated animals. Scale bars = 500 nm. Data shown are the mean±SEM for each group. *$p<0.005$, Apo relative to saline,Tukey's HSD.

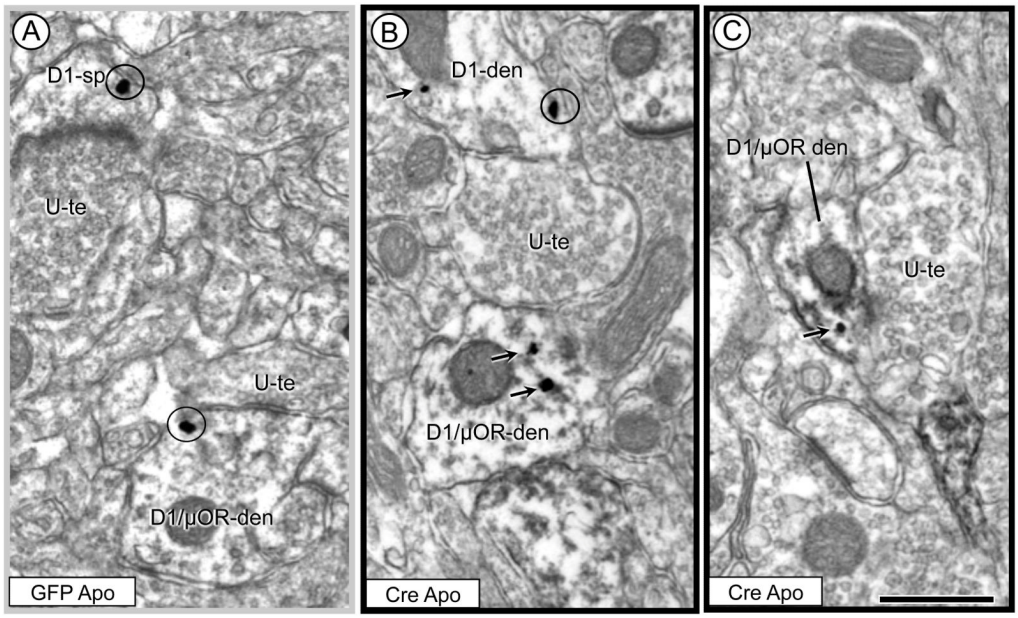

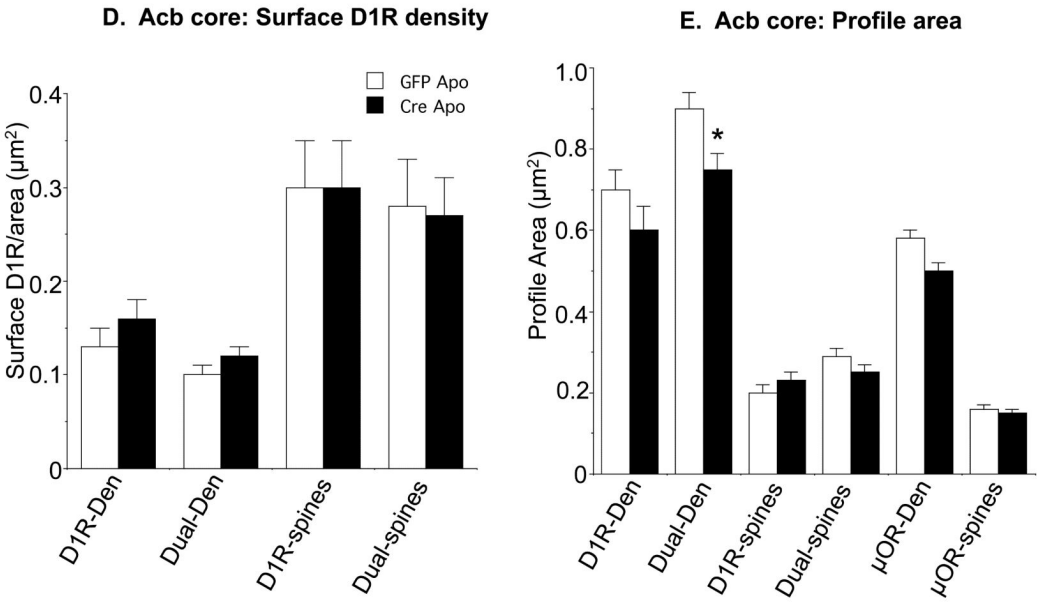

Figure 4.

Single and dual labeled dendrites and spines in the Acb core of mice receiving local injections of rAAV-GFP (n=3) or rAAV-Cre (n=3) and treated with apomorphine (Apo) and AS. Electron microscopic images **(A-C)** show plasmalemmal (circles) and cytoplasmic (arrows) immunogold labeling in D1R (D1-den) and dual labeled dendrites (D1/μ-OR-den), as well as a single D1R labeled spine (D1-sp). Bar graphs in **D** and **E** quantitatively confirm that there is no difference in the density of surface D1R or spine size in Acb neurons of apomorphine treated mice after local NR1 deletion. However, there is a significant decrease in the size of dual labeled dendritic profiles in the Acb of NR1 KO mice given apomorphine.

Scale bars = 500 nm. Data shown are the mean±SEM for each group. *$p<0.05$ in Cre Apo relative to GFP Apo groups by Tukey's HSD.

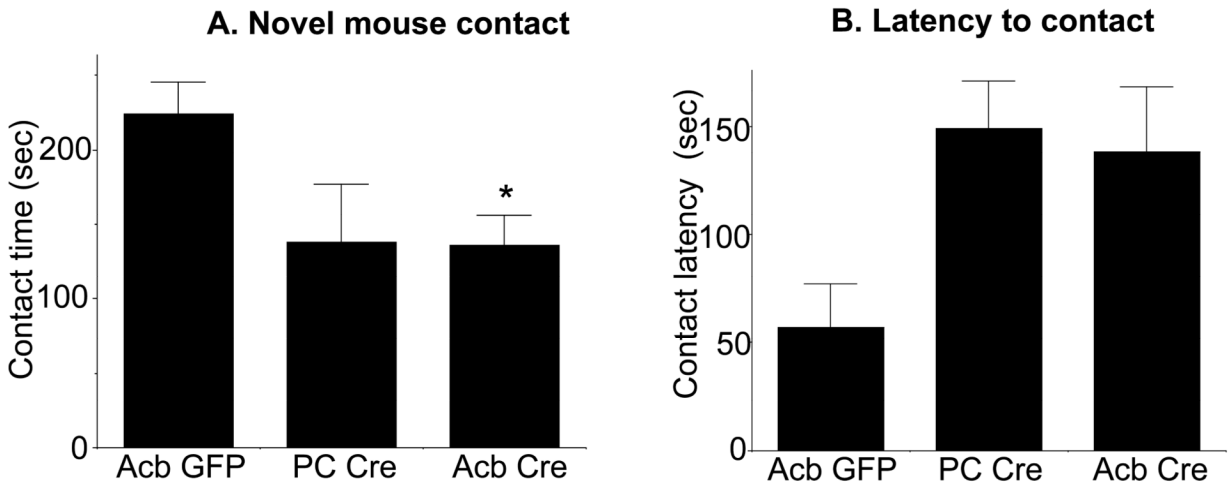

Figure 5.

Acb NR1 deletion impairs sociability. Mice injected with rAAV-Cre bilaterally in the Acb (Acb Cre) differ in sociability when compared to those receiving Acb rAAV-GFP (Acb GFP) but not rAAV-Cre outside the Acb (i.e. placement control [PC] Cre). As shown in **A**, mice receiving Cre in the Acb (n=11) show significantly less contact time with a novel mouse relative to animals receiving Acb GFP (n=5), however Acb GFP mice do not differ from the PC Cre group (n=3). Acb Cre-injected mice also have longer latencies to initiate contact with the novel mouse relative to Acb GFP treated animals **(B)**, although this fails to achieve statistical significance. *$p<0.05$ Acb Cre relative to Acb GFP by Fisher's PLSD.

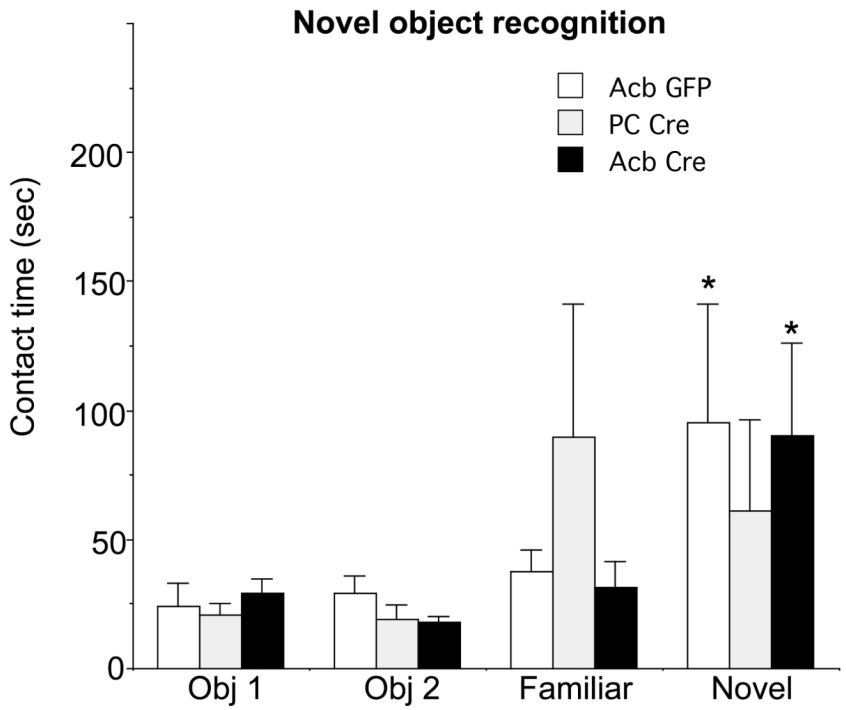

Figure 6.

Contact time with familiar and novel objects during a two-choice novel object recognition test in Acb Cre (n=11), Acb GFP (n=5), and PC Cre mice (n=3). Contact time with objects one (Obj 1) and two (Obj 2) during the familiarization step are presented at the left and subsequent contact time with one of the latter objects (Familiar) and a new object (Novel) during the test phase are presented at the right. None of the groups differed in the amount of time spent with each of the two objects during the familiarization stage. Mice receiving Acb Cre or Acb GFP spend significantly more time engaged with the novel object during the test phase. The PC Cre mice spend similar amounts of time with both objects. *$p<0.05$ Acb Cre relative to Acb GFP in contact with a novel versus familiar object in Acb GFP and Acb Cre mice by Fisher's PLSD.

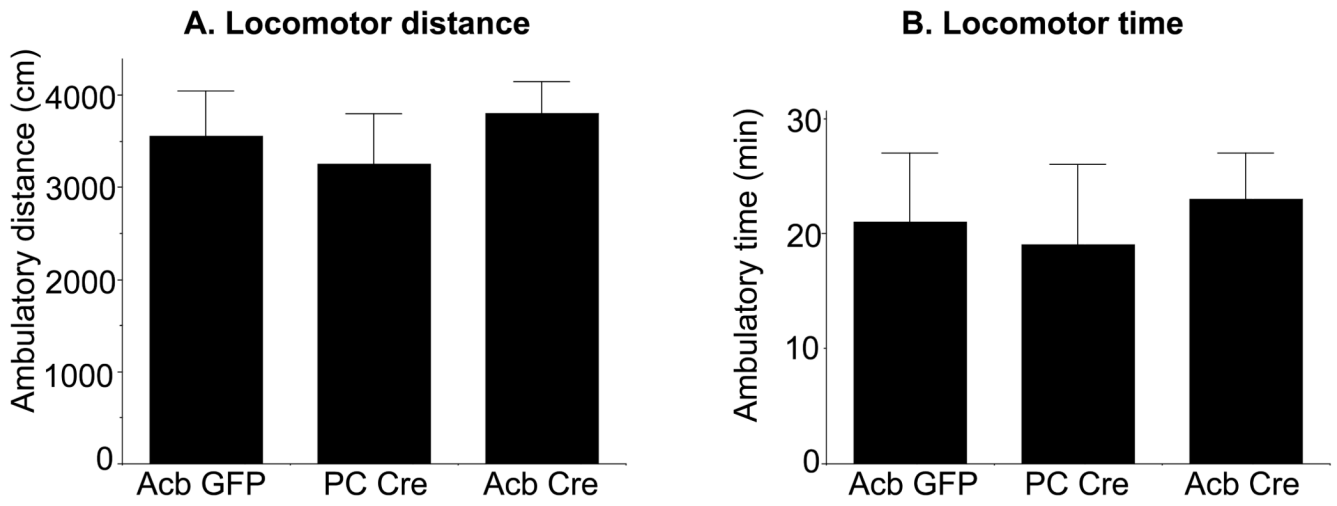

Figure 7.

Open field behavior in Acb NR1 KO and control mice. rAAV-Cre injected (Acb Cre n=11) and control (Acb GFP n=5, and PC Cre n=4) mice display no significant differences in locomotor activity as measured by either distance traveled **(A)** or activity time **(B)** in an automated open field. Data shown are the mean±SEM for each group.

Table 1

Combination of Treatments and Number of mice used for electron microscopic analysis

Unilateral Acb Injections rAAV-Cre NR1-KO or rAAV-GFP	Injection Location	Drug treatment	Animal Number
rAAV-GFP	Acb Core	Saline	3
rAAV-Cre	Acb Core	Saline	3
rAAV-GFP	Acb Core	Apomorphine	3
rAAV-Cre	Acb Core	Apomorphine	3
rAAV-GFP	Acb Shell	Saline	3
rAAV-Cre	Acb Shell	Saline	3
rAAV-GFP	Acb Shell	Apomorphine	3
rAAV-Cre	Acb Shell	Apomorphine	4

All mice were allowed to recover for 14 days after the viral injections, and then were given s.c injection of saline or apomorphine (5mg/kg) five minutes before the AS and PPI testing and 1 hr prior to being anesthetized and having their brain tissue fixed by cardiac perfusion for electron microscopic immunolabeling.

Table 2
Treatments and Number of mice used for behavioral studies

Bilateral Injections rAAV-Cre NR1-KO or rAAV-GFP	Injection Location	Animal Number
rAAV-GFP	Acb	5
rAAC-Cre	Outside Acb	3
RAAV-Cre	Acb	11

Mice were subject to a battery of behavioral tests including locomotor activity, sociability, and novel object recognition 14 days following viral injections.